Advanced Robotics

ISSN: 0169-1864 (Print) 1568-5535 (Online) Journal homepage: http://www.tandfonline.com/loi/tadr20

Muscle synergy structure using different strategies in human standing-up motion

Ningjia Yang, Qi An, Hiroshi Yamakawa, Yusuke Tamura, Atsushi Yamashita & Hajime Asama

To cite this article: Ningjia Yang, Qi An, Hiroshi Yamakawa, Yusuke Tamura, Atsushi Yamashita & Hajime Asama (2017) Muscle synergy structure using different strategies in human standing-up motion, Advanced Robotics, 31:1-2, 40-54, DOI: 10.1080/01691864.2016.1238781

To link to this article: http://dx.doi.org/10.1080/01691864.2016.1238781

ADVANCED ROBOTICS, 2017
VOL. 31, NOS. 1–2, 40–54
http://dx.doi.org/10.1080/01691864.2016.1238781

RSJ Taylor & Francis
Taylor & Francis Group

FULL PAPER

Muscle synergy structure using different strategies in human standing-up motion

Ningjia Yang, Qi An, Hiroshi Yamakawa, Yusuke Tamura, Atsushi Yamashita and Hajime Asama

Department of Precision Engineering, The University of Tokyo, Tokyo, Japan

ABSTRACT

Standing-up motion is an important daily activity. It has been known that humans can employ different strategies to stand up from a chair, but it was not clear how people control their redundant muscles to achieve different strategies. This study employs the concept of muscle synergy which suggests that humans utilize the small number of modules (called muscle synergy) to generate the movements. This study uses two approaches to understand how humans generate different movements. Firstly, measurement experiment was performed to investigate the muscle synergy structure during different strategies. Next, the finding from the measurement experiment is validated through the forward dynamic simulation using our developed neuromusculoskeletal model. Both of our results from simulation study and measurement experiment showed that four muscle synergies could generate standing-up motion. However, they adaptively changed the start time of a certain synergy to achieve different strategies.

ARTICLE HISTORY
Received 18 April 2016
Revised 18 June 2016
Accepted 18 August 2016

KEYWORDS
Muscle synergy; standing-up motion; motion analysis

1. Introduction

In the past decades, the world's elderly population has been increasing sharply. According to United Nations, the proportion of the world's population aged 60 years or over increased from 8% in 1950 to 12% in 2013, and it is estimated that it will increase more rapidly to reach 21% in 2050.[1] In order to improve the quality of life of the elderly, the standing-up motion is focused. Standing-up motion is one of the most common daily activities, which also influences other activities.

In robotic research, many kinds of devices and robots were developed to assist standing-up motion. Chugo et al. [2] developed an assistive system which was composed of a bed and a bar to lead human body to follow the desired trajectory. Agrawal et al. [3] proposed a chair-type device using gravitational force to lift up the hip of the user to help people accomplish standing-up motion. A robotic exoskeleton assistive system was developed to support the user's standing-up motion synchronizing his or her intention.[4] In addition, a sit-to-stand trainer which aimed to support or to train sit-to-stand motion was developed based on kinematics, kinetics and EMG patterns of standing-up motion.[5] In order to take full advantage of these devices and help the humans stand up, it is necessary to clarify the mechanism of the standing-up motion.

To understand the mechanism of the standing-up motion, it is important to understand how humans achieve varied movement. Essentially, human movement is varied because human body is a redundant system where there are more muscles than the number of joints to be controlled. Hughes et al. [6] defined three strategies (momentum transfer, stabilization, and hybrid) used in humans standing-up motion which generate different movements. They found that younger persons tend to use the momentum transfer strategy which utilizes the momentum to lift up their body. On the other hand, the elderly persons tend to use the stabilization strategy in which they carry their center of mass (CoM) first on their feet and then they move upward. The hybrid strategy is the middle between momentum transfer and stabilization. Other studies also compare the standing-up motion between the young and the elderly. They found that the older adults showed more vastus lateralis (VAS) muscle activity, greater knee flexion and greater trunk forward lean than young adults.[7] However, they could not reveal how humans control redundant muscles to generate standing-up motion.

In order to clarify how humans coordinate their redundant number of muscles to generate different standing-up movements, the concept of muscle synergy has been employed in the area of human motor control theory. Muscle synergy was firstly proposed by Bernstein, which suggested that human movements could be generated from a limited number of modules (called muscle synergy).[8] It claimed that humans did not control individual muscles, but they controlled modules of muscles. Muscle synergy theory decomposes the complex control of individual muscles into modular organization.

CONTACT Ningjia Yang yang@robot.t.u-tokyo.ac.jp

Previous studies showed human movements such as locomotion, posture control and hand posture could be explained by a small number of muscle synergies.[9–11] Ivanenko et al. [9] found that muscle synergy structure changed little when humans walked with different speeds and gravitational loads, but they adaptively changed the weighting coefficient of muscle synergy to achieve different locomotion. In human postural control, it was also found that muscle synergies were similar while muscle synergy coefficient changes with different posture.[10] These findings suggested that humans might utilize different combinations or different ways to activate the limited number of muscle synergies to accomplish adaptive movements. In addition, a previous study [12] analyzed changes in muscle coordination with training and the results showed that there was possibility that the plasticity exists by the repetitive execution of movement patterns which were supported by intrinsic muscle synergies. This result also suggested that clarification of muscle synergy structure is necessary in rehabilitation.

In our previous study,[13] a neuromusculoskeletal model was developed to simulate how muscle synergies contribute to the standing-up motion. Previous studies also employed simulation model to analyze how muscle synergy contribute to human movement.[14,15] Aoi et al. used the similar neuromusculoskeletal model to analyze how phase resetting affected human bipedal walking. Jo et al. employed cerebrocerebello-spinomuscular interaction model to analyze how to generate stable long-loop walking. Our simulation study implied the possibility that changing parameters of muscle synergies could generate different trajectories of the motion. However, the simulation study used a specific muscle synergy patterns which were extracted from only one subject. Therefore, we perform the measurement experiment in this study to investigate the muscle synergy structure among different strategies of human standing-up motion. Although the measurement experiment can give the necessary condition to achieve the motion, it was still unclear whether the condition also satisfies the essential condition for the movement achievement. In order to elucidate the essential condition, we use our developed neuromusculoskeletal model to perform the forward dynamic simulation to verify the results from the measurement experiment. In this study, our objective is to clarify muscle synergy structure in different strategies of standing-up motion. In particular, firstly the measurement experiment is conducted to find muscle synergy structure. Next, the finding will be validated through the forward dynamic simulation.

2. Muscle synergy model

In this section, muscle synergy model is explained. Bernstein suggested that human movement was composed of the small sets of modules (called synergy). It assumes humans do not control individual muscles but they control group of muscles. The muscle synergy model has been widely used to analyze human movements.[9,10] For the muscle synergy model, muscle activation can be expressed as a linear summation of spatiotemporal patterns in a mathematical expression, as in Equation (1),

$$\mathbf{M} = \mathbf{WC}, \tag{1}$$

where $\mathbf{M}$, $\mathbf{W}$, and $\mathbf{C}$ indicate muscle activation, spatial pattern and temporal pattern matrices respectively. Matrix $\mathbf{M}$ consists of the muscle activation vectors $\mathbf{m}_{i(i=1,2,\ldots,n)}$ to represent n different muscle activations (Equation (2)).

$$\begin{aligned}\mathbf{M} &= \left(\mathbf{m}_1(t)\ \mathbf{m}_2(t)\ \ldots\ \mathbf{m}_n(t)\right)^T \\ &= \begin{pmatrix} m_1(1) & \ldots & m_1(t_{\max}) \\ \vdots & \ddots & \vdots \\ m_n(1) & \ldots & m_n(t_{\max}) \end{pmatrix}.\end{aligned} \tag{2}$$

The components of the vector $m_i(t)$ represent discrete i-th muscle activation at time t ($1 \leq t \leq t_{\max}$). Variable n represents the number of muscles. Spatial pattern $\mathbf{W}$ is used to represent the relative activation level of muscle. Variable N indicates the number of muscle synergies. Its column shows N different spatial pattern vectors $\mathbf{w}_{j(j=1,2,\ldots,N)}$. The vector $\mathbf{w}_j$ consists of w_{ij} which represents relative activation level of muscle i included in j-th muscle synergy (Equation (3)).

$$\begin{aligned}\mathbf{W} &= \left(\mathbf{w}_1\ \mathbf{w}_2\ \ldots\ \mathbf{w}_N\right) \\ &= \begin{pmatrix} w_{11} & \ldots & w_{1N} \\ \vdots & \ddots & \vdots \\ w_{n1} & \ldots & w_{nN} \end{pmatrix}.\end{aligned} \tag{3}$$

Temporal pattern $\mathbf{C}$ is used to indicate the weighting coefficient of N muscle synergies (Equation (4)). Its row shows N different temporal pattern vectors $\mathbf{c}_j(j = 1, 2, \ldots, N)$, which indicate temporal pattern corresponded to the spatial patterns $\mathbf{w}_j$. Its components are $c_j(t)$, which represent weighting coefficient of j-th muscle synergy at time t.

$$\begin{aligned}\mathbf{C} &= \left(\mathbf{c}_1(t)\ \mathbf{c}_2(t)\ \ldots\ \mathbf{c}_N(t)\right)^T \\ &= \begin{pmatrix} c_1(1) & \ldots & c_1(t_{\max}) \\ \vdots & \ddots & \vdots \\ c_N(1) & \ldots & c_N(t_{\max}) \end{pmatrix}.\end{aligned} \tag{4}$$

Figure 1 shows a schematic design of muscle synergy model. Three muscle synergies are used to express n muscle activations. They are composed of spatial and

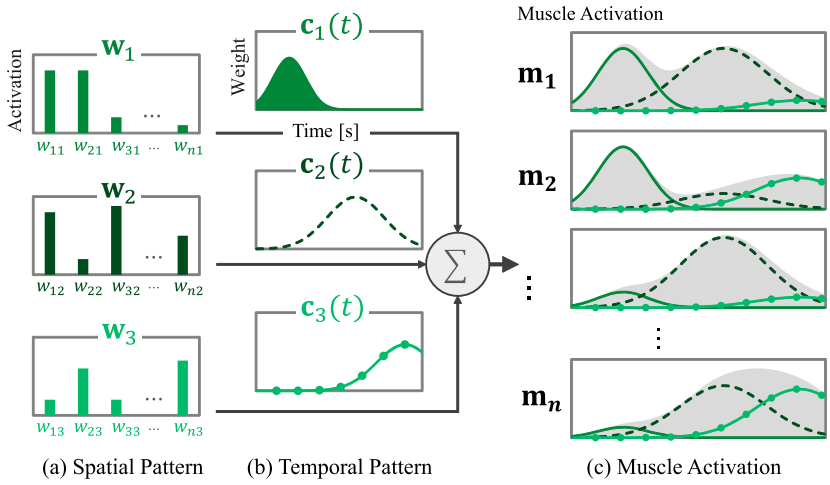

Figure 1. Muscle synergy model. (a) shows spatial patterns ($\mathbf{w}_{1,2,3}$) which represents the activation level of related muscles. (b) shows temporal patterns ($\mathbf{c}_{1,2,3}$) to indicate the time-varying weighting coefficient of corresponding muscle synergies. (c) shows time-varying activation of n muscles (gray part). The solid, dashed, and circle lines show the generated muscle activation from muscle synergies 1, 2, and 3 respectively.

temporal patterns. Spatial patterns ($\mathbf{w}_{1,2,3}$) show relative muscle activation level. Temporal patterns ($\mathbf{c}_{1,2,3}$) show the relative weighting coefficients. During the mot ion, spatial patterns are constant, but temporal patterns change according to the time. Muscle activations are generated from linear summation of spatial and temporal patterns of muscle synergies. Muscle activations are shown in gray areas and muscle synergies 1, 2, and 3 are described in solid lines, dashed lines, and solid lines with circles in Figure 1.

To calculate elements of the matrices $\mathbf{W}$ and $\mathbf{C}$, nonnegative matrix factorization (NNMF) [16] was used. Firstly, the initial elements of matrix $\mathbf{W}$ are decided randomly. Secondly, the matrix $\mathbf{C}$ is solved using Equation (5). Thirdly, the matrix $\mathbf{W}$ can be solved by Equation (6). By repeating Equations (5) and (6), matrices $\mathbf{W}$ and $\mathbf{C}$ can be obtained.

$$\mathbf{W}^{\mathrm{T}}\mathbf{W}\mathbf{C} = \mathbf{W}^{\mathrm{T}}\mathbf{M}, \tag{5}$$

$$\mathbf{C}\mathbf{C}^{\mathrm{T}}\mathbf{W}^{\mathrm{T}} = \mathbf{C}\mathbf{M}^{\mathrm{T}}. \tag{6}$$

3. Measurement experiment

In this study, firstly the measurement experiment is conducted to clarify the muscle synergy structure during different strategies of human standing-up motion. In the experiment, body trajectory, reaction force, and muscle activation are measured, and muscle synergy structure is mainly determined from muscle activation data. Details of our experiment are explained below.

3.1. Experimental protocol

In this experiment, subjects are asked to stand up usi ng two different strategies (momentum transfer and stabilization) intentionally. Before starting the experiment, an experimenter explains the characteristics of the strategies to each participant. When they perform the motion, we ask them to locate their feet 80° from the horizontal direction at the initial state of the experiment. Additionally, they are told to cross their arms in front of their chest to avoid using the arms. The chair height was adjusted to the height of the subject's lower leg. The subjects finished the motion without moving feet in all the trials. Recording time for each trial is 10 s. Experiment environment is shown in Figure 2(a).

This experiments measured 10 muscles as following: tibialis anterior (TA), gastrocnemius (GAS), soleus (SOL), rectus femoris (RF), vastus lateralis (VAS), biceps femoris long head (BFL), biceps femoris short head (BFS), gluteus maximus (GMA), rectus abdominis (RA), and erector spine (ES). These muscles were chosen because they either contribute to the flexion and extension of the ankle, knee, hip, and lumbar joints. These muscle positions are shown in Figure 2(b) and (c).

In this experiment, 11 healthy male subjects (24.5 ± 2.2 years old, 1.73 ± 0.03 m, 60.1 ± 2.4 kg) were asked to participate at our experiment. For each strategy, there were 15 trials. The informed consent was obtained from all participants according to the protocol of the Institute Review Board of The University of Tokyo.

3.2. Experimental setup

In this experiment, motion capture system (Motion Analysis. Corp.) was used to obtain the kinematics information of the subject in 100 Hz. This motion capture system had eight infrared cameras. Human body positions are measured based on Helen Hayes marker set. Joint

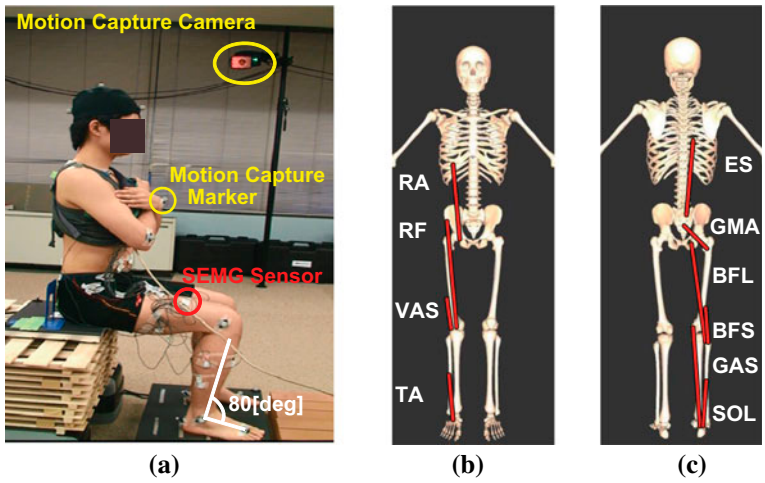

Figure 2. Experimental Environment. (a) An optical motion capture system, force plates, and sEMG sensors are used to record kinematics, dynamics, and muscle activation data. (b) Measured muscles are shown above from front view. (c) Measured muscles are shown above from back view.

angle data were calculated using SIMM (Musculographics, Inc.) based on the joint position data. Surface EMG device (DL-141, S&ME Corp.) was used in this experiment to get muscle activities data in 1000 Hz. Two force plate devices (TechGihan. Corp.) were used to get the reaction force data in 1000 Hz.

3.3. Data preprocessing

In this study, all the recorded data were filtered. Muscle activation data was filtered with a band pass filter of 60–200 Hz to remove noise and the moving average was calculated for 1.0 s before and after the data point. The joint position data were filtered with the second-order Butterworth low pass filter with 5 Hz. The collected reaction force data were filtered with low pass filter of 20 Hz.

The duration time of the standing-up motion is different among different trials and subjects. In order to compare different trials, the duration time needs to be normalized. To normalize the duration time, the standing-up motion is divided into four phases.[17] The start time of phase 1 is set as the start of standing-up motion. The start time of phase 1 is when the horizontal velocity of shoulder exceeds 0.2 m/s. Phase 2 is when the hip leaves the seat. The start time of phase 2 is when the vertical reaction force of hip is less than 0 N. Phase 3 is the time when the subjects start to move upward. The start time of phase 3 is when the horizontal displacement of the knee gets its maximum. The start time of phase 4 is when the vertical velocity of shoulder becomes less than 0.1 m/s after the start time of phase 3. The end time of phase 4 is set as the end of the motion. However, the end time cannot be defined clearly since humans just stand straight in the end of the standing-up motion. Therefore, the duration of phase 4 is decided as to the 25% of the duration time from phases 1–3. The recording data were cut based on the start time of phase 1 and the end time of phase 4. Then, the motion time is normalized to 100%.

When all the data were obtained, muscle synergies were extracted from muscle activation data using NNMF. To test whether muscle synergy can well represent muscle activation, the determination of coefficient R^2 is calculated. In addition, in order to decide the number of muscle synergies, one-factor analysis of variance (ANOVA) is employed to evaluate how additional synergies affect the performance of muscle synergies. When there is a statistic significance, a post hoc test is applied to the neighbouring number of synergies to evaluate if additional muscle synergies can increase the performance. The statistical significant level p is set to be 0.05.

In order to investigate whether humans utilize the same muscle synergies among different strategies, the cosine similarity among spatial patterns are calculated. The similarity s_{ij} between muscle synergies $\mathbf{w}_i$ and $\mathbf{w}_j$ is obtained from the following equation,

$$s_{ij} = \frac{\mathbf{w}_i \cdot \mathbf{w}_j}{|\mathbf{w}_i||\mathbf{w}_j|}. \tag{7}$$

3.4. Results of measurement experiment

3.4.1. Verification of recorded motion

In order to verify whether the participants stood up using the right strategies as we required, the CoM was calculated. In order to calculate the CoM trajectory, the same four-link model was used as our previous study.[13] The previous study [8] defined that the horizontal velocity of CoM using stabilization and momentum transfer strategies are less than 0.075 m/s and more than 0.1 m/s

respectively. Our obtained results satisfied the definition and verified that the subjects could perform different strategies in our experiment.

Figure 3 shows CoM trajectories of different strategies. Horizontal and vertical axes indicate normalized CoM displacement. The displacement was normalized based on the height of each subject. Solid and dashed lines indicate CoM trajectory of the momentum transfer and the stabilization strategies respectively. The gray area on the horizontal axis shows feet support area. This result shows that when the subject used the momentum transfer strategy, the vertical CoM increased directly as the horizontal CoM increases. However, when the subject used the stabilization strategy, the vertical CoM decreases first when the horizontal CoM increases. This is because the subject firstly moved the CoM on their feet. Then the vertical CoM increases as the subject begins to move upward. While in the stabilization strategy, the stimulated CoM started to move forward firstly, then began to move upward.

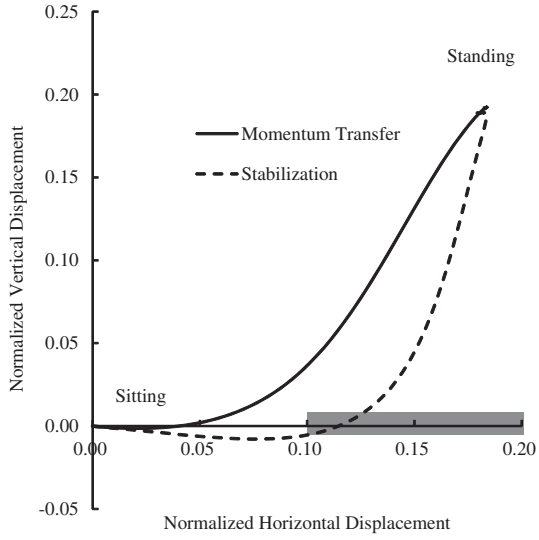

Figure 3. CoM trajectory. Center of mass trajectories of two strategies are depicted above. The vertical and horizontal axes indicate normalized displacement in each direction. The gray area on the horizontal axis shows foot support area. This result indicates that humans move upward even before their CoM is on the feet in the momentum transfer strategy. On the other hand, humans start moving upward after their CoM is on the feet.

3.4.2. The number of muscle synergies

In order to decide the number of muscle synergies, coefficient of determination R^2 was calculated. Figure 4 shows the coefficient of determination R^2 of different number of muscle synergies. The solid and dashed lines, respectively, represent momentum transfer and stabilization strategies. As a result of ANOVA, there was a statistical significance in the coefficient of determination R^2 based on the number of muscle synergies (momentum transfer: $F = 1121.44$, $p < 0.05$, Stabilization: $F = 563.97$, $p < 0.05$). Post hoc test indicated that there was a significant difference in the number of muscle synergies between one and two, two and three, and three and four ($p < 0.05$). This indicated that the coefficient of determination R^2 significantly increased until the muscle synergy number was four. In addition, the result showed that four muscle synergy could represent 94 and 93% muscle activation in momentum transfer and stabilization strategies respectively.

3.4.3. Spatial and temporal patterns of muscle synergies

Figure 5(a), (c), (e) and (g) show the spatial patterns of four muscle synergies which are used to explain muscle activation of the ten selected muscles. Black and white bars show relative muscle activation when subjects used momentum transfer and stabilization strategies, respectively. Each synergy had particular contribution to body movements according to human anatomy. In Figure 5(a), it shows that muscle synergy 1 mostly activated RA which flexed the lumbar and produced momentum necessary for the standing-up motion. Muscle synergy 2 mostly activated TA which dorsiflexed the ankle joint to move CoM forward, and activated VAS and RF to extend the knee, as Figure 5(c) shows. In Figure 5(e), muscle synergy 3 mainly activated ES and VAS to extend trunk and knee, which lift up the whole body Figure 5(g) shows that muscle synergy 4 activated GAS and SOL, which flexes knee and ankle to decelerate movement of CoM. Similarity between the each muscle synergies of the two strategies was quantified using the cosine principal angles. Similarity represents the dimensionality of the subspace shared between the spaces spanned by the muscle synergy sets of the two strategies.[18] In addition, the previous study [18] set the threshold of similarity as 0.90. In our study, the similarities between each synergies were found to be 0.95, 0.99, 0.99, and 0.99 for synergies 1, 2, 3, and 4, respectively. In order to validate that the same spatial patterns can actually generate different strategies, forward dynamic simulation is used. The detailed procedure will be explained in the next section.

Figure 5(b), (d), (f), and (h) show the temporal pattern of the four muscle synergies. The vertical lines in the graphs show the start time of the phases 1–4. The start time of each phase is shown in Table 1. Since the start time of the phase 1 was decided as the start of the motion, it is set to be 0%.

The weighting coefficient of temporal pattern is on the vertical axis. The duration time of the whole standing-up motion is on the horizontal axis, and the time was normalized to 100%. The black solid and dashed lines show the temporal patterns of momentum transfer and stabilization strategies. In Figure 5(b), muscle synergy

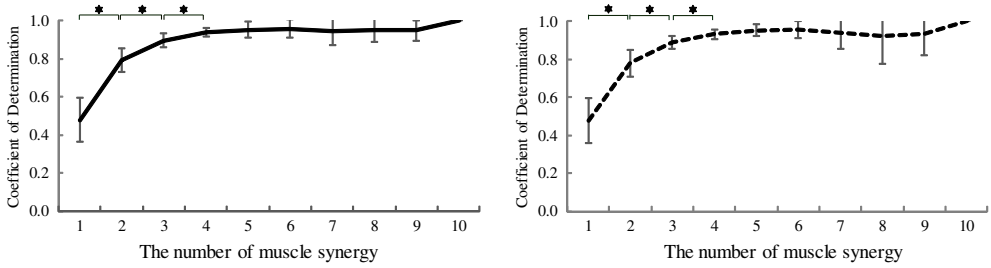

Figure 4. Coefficient of determination. Above two figures show how the coefficient of determination R^2 is changed according to the number of muscle synergies when standing-up using the two strategies. Both the two figures show that statistical significance increased until the number of muscle synergies is four.

Table 1. Onset Time of Four Phases. Below shows start time of each phases among two strategies.

	Phase 2	Phase 3	Phase 4
Momentum Transfer	33%	46%	80%
Stabilization	32%	47%	80%

1 was firstly activated during the phase 1 to bend upper trunk. Figure 5(d) shows that muscle synergy 2 was activated next and it had the peak at the phase 2 to lift up the hip. The main characteristic difference can be found in this synergy. The momentum transfer strategy activated the muscle synergy 2 earlier than the muscle synergy 3. Figure 5(f) shows that synergy 3 started to activate muscles thirdly to move body upward at the phase 3 to extend their whole body. Figure 5(h) shows that it activated GAS and SOL to flex the ankle and knee joints at the phase 4 to decelerate their horizontal CoM movement and keep balance.

From this measurement experiment, it was implied that humans would utilize the similar spatial patterns. Also, their temporal patterns were similar each other between two strategies except the muscle synergy 2. The muscle synergy 2 was activated earlier in the momentum transfer strategy than the stabilization strategy. This implied that humans adaptively changed the start time of the synergy 2 to lift up the hip earlier to utilize the momentum. On the other hand, the stabilization strategy had the delayed lifting up time until they moved their CoM onto the feet.

3.4.4. Joint kinematics

Figure 6 shows the ankle, knee, hip, and lumbar joint angles, respectively. Black solid and dashed lines represent the joint angles change during the standing-up motion of the momentum transfer and stabilization strategies respectively. The vertical direction shows the angles in radian. The horizontal direction shows the motion process (normalized motion time). Figure 6(c) and (d) represent that hip and lumbar joints have larger amplitude when using stabilization strategy. These results indicated that the subjects need to bend their body more to move their CoM forward when using stabilization strategy. In addition, the subjects dorsiflexed their ankle to carry the body forward.

4. Simulation experiment with neuromusculoskeletal model

From the measurement experiment explained above, it has been implied that humans could generate the different strategies of standing-up motion using the same synergies. On the other hand, it was shown that they changed the specific parameters of the synergy. However, this measurement experiment only gives a necessary condition to achieve the movement. Therefore, in this section, we conduct a simulation study to verify our finding from the experiment. In the simulation study, the neuromusculoskeletal model is used to investigate whether different strategies are realized only by changing the start time of the synergies.

4.1. Neuromusculoskeletal model

In order to evaluate the effect of parameter change of the muscle synergy, neuromusculoskeletal model is used and forward dynamic simulation is performed. Our developed system consists of nervous system and musculoskeletal model as shown in Figure 7. Firstly, the nervous system generates motor command u from the muscle synergy model, and the postural control generates joint torque $\mathbf{T}_{\mathrm{fb}}$ to stabilize body posture. Next, the muscle model generates muscular tension and it is converted to the joint torque $\mathbf{T}_{\mathrm{mus}}$ from motor command u. Finally, skeletal model calculates body posture from joint torque, joint property, and interaction force from floor. Details of each parts are described below.

4.1.1. Nervous system

The nervous system has two components such as muscle synergy model to generate motor command and postural

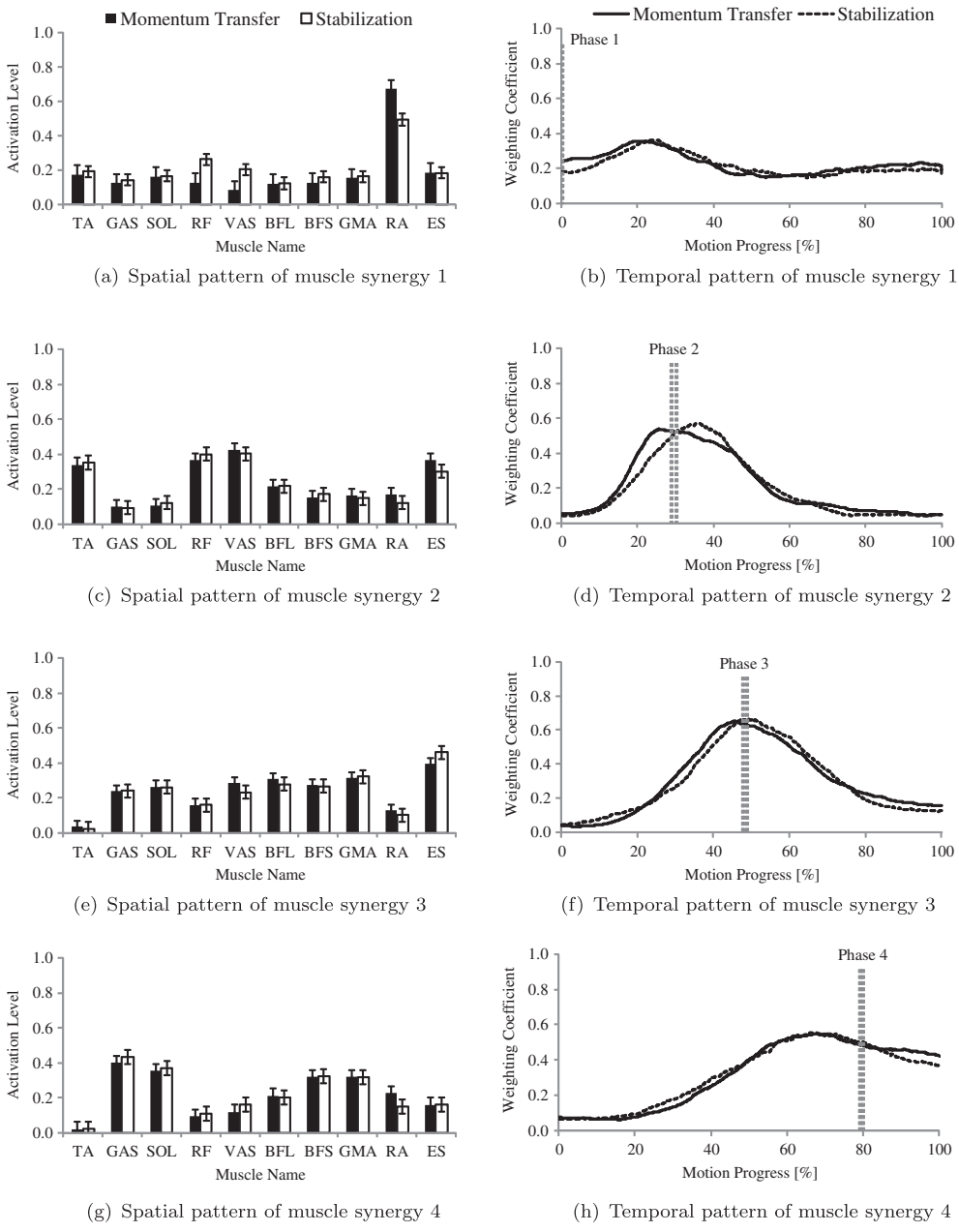

Figure 5. Spatiotemporal patterns of four muscle synergies. Figure 5(a), (c), (e), (g) show the spatial patterns of the four muscle synergies. Above bars show the relative activation level of muscles. Figure 5(b), (d), (f), (h) show the time-varying weighting coefficient of muscle synergyies 1–4.

control to generate joint torque to stabilize the posture. In the simulation study, muscle synergy model generates motor command u (not muscle activation) from spatial pattern $\mathbf{W}$ and time-varying weight $\mathbf{C}$. In order to decide spatial patterns of muscle synergy model, firstly joint torques are computed with the same four-link model by inverse dynamic calculation using body trajectories and reaction force in the previous measurement experiment in Section 3. Next, joint torque is used to determine the amount of muscular tension necessary to achieve the standing-up motion. Then, muscle activation m_i is decided from the muscular tension, but it cannot be determined uniquely since our model includes bi-articular muscles (GAS, RF, and BFL). In addition, one inner muscle is included in the model although it cannot be measured from the experiment. To solve these problems, optimization methodology is utilized to decide muscle activation m_i' to minimize the following squared error z,

$$z = \frac{1}{2}\sum_{i=1}^{N} ||m_i' - m_i||^2. \tag{8}$$

NNMF is applied to the muscle activation m_i' to obtain spatial pattern $\mathbf{w}$. In the simulation study, square

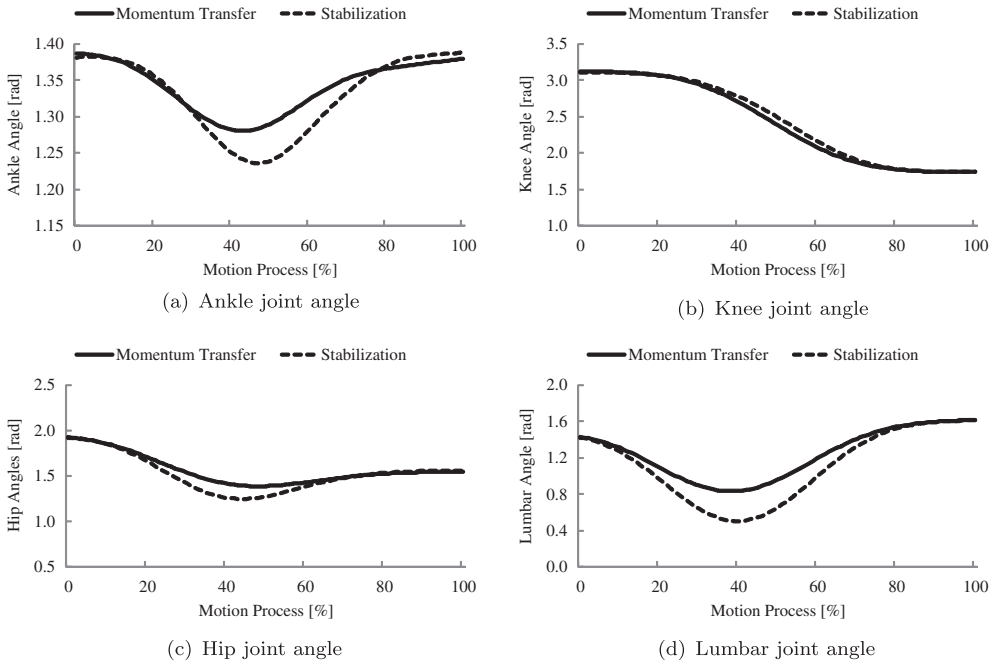

Figure 6. Measured joint angles. Figure 6(a)–(d) show ankle, knee, hip, and lumbar joint angles, respectively.

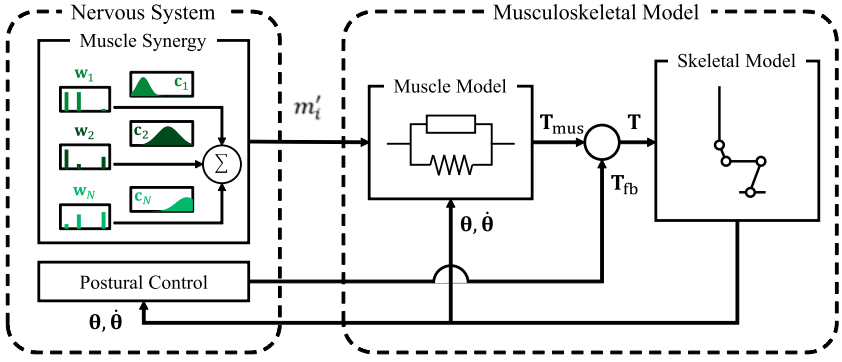

Figure 7. Above figure shows schematic diagram of our neuromusculoskeletal model. Nervous system consists of muscle synergy model and posture control; the muscle synergy model generates motor command u and postural control generates a joint torque $\mathbf{T}_{\mathrm{fb}}$ to stabilize the body posture. On the other hand, the muscle model receives motor command u to calculate joint torque $\mathbf{T}_{\mathrm{mus}}$. When summation of both torques $\mathbf{T}_{\mathrm{mus}}$ and $\mathbf{T}_{\mathrm{fb}}$ are input to the skeletal model, it calculates body posture Θ and $\dot{\Theta}$. Body postures are fed back to the postural control and the muscle model as well.

wave is used to represent time-varying weight $\mathbf{c}$. We use square waves to avoid the effect of the noise from surface electromyography. Essentially surface electromyography includes the noise due to skin condition, hair, and signal decay, and therefore m_i' is affected by the noise as well. Therefore, in order to reduce the effect of the noise, square wave is employed in this study. Their rising time and duration are arbitrarily decided by trying and error. When motor command is input to the muscle model, it is converted into the muscle activation using first-order differential equation explained in the later section.

In addition to the muscle synergy model, postural control is used to stabilize the posture of the skeletal model. It generates joint torque $\mathbf{T}_{\mathrm{fb}}$ by the proportional control to each joint based on the error of joint angles between the measured ones in Section 3 and the ones in simulation. It is obtained from the following equations,

$$\mathbf{T}_{\mathrm{fb}} = \mathbf{K}^{\mathrm{q}}\Delta\mathbf{q}(t) + \mathbf{K}^{\dot{\mathrm{q}}}\Delta\dot{\mathbf{q}}(t) + \mathbf{K}^{\ddot{\mathrm{q}}}\Delta\ddot{\mathbf{q}}(t), \quad (9)$$

$$\Delta x(t) = \hat{x}(t-\lambda) + x(t-\lambda), \quad (10)$$

where parameters $\Delta\mathbf{q}(t)$, $\Delta\dot{\mathbf{q}}(t)$, $\Delta\ddot{\mathbf{q}}(t)$ represent joint angle, angular velocity and acceleration, and vectors $\mathbf{K}^{\mathbf{q},\dot{\mathbf{q}},\ddot{\mathbf{q}}}$ show coefficients for joint angle, angular velocity and acceleration in the proportional control. Time delay λ is taken into account as a nervous transmission delay. Also, the maximum and minimum joint torque is limited to ± 50 Nm. This limitation is to mainly evaluate the effect of muscle synergies.

4.1.2. Skeletal model

In this study, human body is represented with four segments; an upper trunk, a pelvis, a thigh, and a shank (Figure 8(a)). When all the segment parameters (mass, segment length, position of CoM, and inertia) are given, an equation of motion is derived as follows:

$$\mathbf{I}(\Theta, \ddot{\Theta}) + \mathbf{h}(\Theta, \dot{\Theta}) + \mathbf{g}(\Theta) + \mathbf{D}(\Theta, \dot{\Theta}) = \mathbf{T} + \Phi(\Theta, \dot{\Theta}), \tag{11}$$

where matrices $\mathbf{I}(\Theta)$, $\mathbf{h}(\Theta, \dot{\Theta})$, and $\mathbf{g}(\Theta)$ indicate inertia term, non-linear term, and gravitational term which could be obtained from Lagrangian equation of motion. Matrix $\mathbf{D}(\Theta, \dot{\Theta})$ indicates joint resistance force according to position and velocity of each joint [19,20]. Parameter k=1, 2, 3, 4 indicate the ankle, knee, hip, and pelvis joints as in the following equation,

$$\mathbf{D} = \begin{cases} d_k \dot{\theta}_k & \text{when } k = 1, 2, 3 \\ d_k^{\text{ext}} \theta_k & \text{when } k = 4 \ \theta_k > 0.0314. \\ d_k^{\text{flex}} \theta_k & \text{when } k = 4 \ \theta_k \leq 0.0314 \end{cases} \tag{12}$$

Matrix $\mathbf{T}$ represents joint torque which is generated from muscles. Matrix $\Phi(\Theta, \dot{\Theta})$ indicates horizontal and vertical reaction forces generated on the hip joint. The feet of the skeletal model are fixed to the ground. These forces are calculated from kinetic and elastic elements.

4.1.3. Muscle model

The muscle model generates joint torque $\mathbf{T}_{\text{mus}}$. Figure 8(b) shows muscles included in our study. In addition to the 10 muscles in the measurement experiment, we additionally considered iliopsoas (IL). It is because IL is important muscle to flex the hip joint, but it cannot be measured using surface electromyography.

Joint torque is calculated from multiplication of muscular tension F_i and moment arm r_{ki} as in Equation (13),

$$\tau_k = \sum_{k=1}^{4} \sum_{i=1}^{11} r_{ki} F_i. \tag{13}$$

In the equation, moment arm r_{ki} is obtained from previous anatomical studies, and muscular tension F_i is obtained from Hill-type muscle model [21]. The Hill model is composed of the contractile element (CE) and the parallel element (PE). CE of ith muscle actively generates muscle tension F_i^{CE} based on muscle dynamics (force–length f_{fl} and force–velocity f_{fv} relationships), intrinsic maximum contraction force $F_i^{\max}$ and muscle activation m_i as in Equation (14).

$$F_i^{\text{CE}} = F_i^{\max} f_{\text{fl}} f_{\text{fv}} m_i. \tag{14}$$

Force–length relationship f_{fl} and force–velocity relationship f_{fv} are expressed as in Equations (15–16).[19,22]

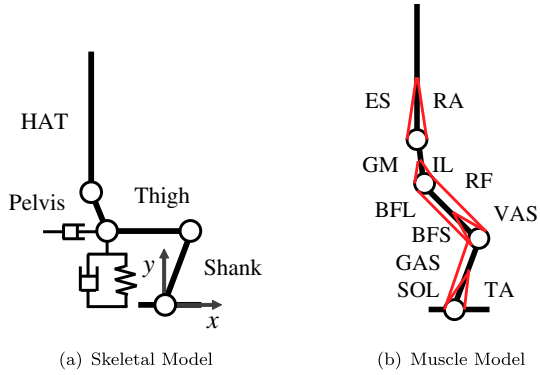

(a) Skeletal Model (b) Muscle Model

Figure 8. Above figure shows musculoskeletal model used in this study. Four segments of shank, thigh, pelvis, and HAT are considered. Eleven muscles are focused including mono- and bi- articular muscles.

Normalized muscular length is calculated from moment arm, current joint angle θ_k and optimal joint angle θ_o as in Equation (17). Similarly, normalized joint angular velocity is obtained as in Equation (18). The normalized muscular velocity $\tilde{v}_i$ assumes that the maximum muscle velocity is equal to 10 times the optimal muscle length [23].

$$f_{\text{fl}} = \exp(-(\tilde{l} - 1)), \tag{15}$$

$$f_{\text{fv}} = 1 + \tanh(\tilde{v}_i), \tag{16}$$

$$\tilde{l}_i = \left(l_i^o + \sum_{k=1}^{4} (r_{ki}(\theta_k - \theta_o)) \right) / l_i^o, \tag{17}$$

$$\tilde{v}_i = \frac{1}{10 l_i^o} \frac{\mathrm{d}l_i}{\mathrm{d}t}. \tag{18}$$

This study employs first-order activation dynamics to calculate muscle activation m_i [24]. When muscles receives motor command u, it does not produce muscle activation directly. The excitation and relaxation dynamics are expressed as in following equation,

$$\frac{\mathrm{d}m}{\mathrm{d}t} = \frac{u - m}{f(m, u)}, \tag{19}$$

$$f(m, u) = \begin{cases} t_{\text{act}}(0.5 + 1.5m) & \text{when } u > m \\ t_{\text{deact}}/(0.5 + 1.5m) & \text{when } u \leq m. \end{cases} \tag{20}$$

Time derivative of muscle activation (dm/dt) is decided from the current activation level m, motor command u and time constant $f(m, u)$. Figure 9 shows the relationship between motor command u and muscle activation m. This converts the square wave form to the non-linear wave pattern as in Figure 9. In our study, muscle activation time t_{act} and deactivation time t_{deact} are set to be 30 and 50 ms, respectively.[24–26]

On the other hand, PE generates passive force F_i^{PE} when the muscle is extended from its optimal length $\tilde{l}_i$

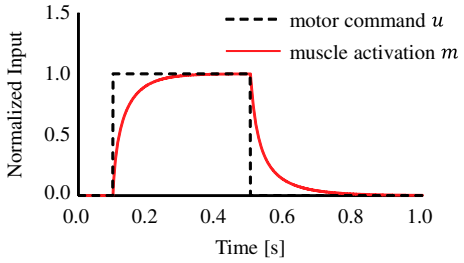

Figure 9. Relationship between input motor command u and muscle activation m. In our study, time constants t_{act} and t_{deact} are set to be 30 and 50 ms respectively.

as in Equation (21).[27] Muscular tension F is obtained summation of contraction force F_i^{CE} and passive force F_i^{PE}.

$$F_i^{PE} = \begin{cases} 0 & \tilde{l}_i \leq 1.0 \\ F_i^{max} \frac{e^{10(\tilde{l}_i)-1}}{e^5} & 1.0 < \tilde{l}_i < 1.5. \\ F_i^{max} & 1.5 \leq \tilde{l}_i \end{cases} \quad (21)$$

4.2. Effect of start time of muscle synergy

Using the developed neuromusculoskeletal model, forward dynamic simulation is performed. Firstly, initial posture is given to the model. Next, muscle activation is calculated from motor command generated in the muscle synergy model. Then the muscle model calculates joint torque generated on each joint. Finally, skeletal model calculates body posture taking floor reaction force and joint resistance force into account. For the numerical calculation, fourth-order Runge–Kutta method is used and time step is set to be 1 ms.

From our measurement experiment, it was implied that humans could employ the similar synergies to generate different strategies of the standing-up motion only by changing specific parameters of them. In order to verify that, forward dynamic simulation is conducted to investigate whether it is possible to generate the different strategies using the same muscle synergies.

In particular, we use the following equation to calculate the motor command u:

$$u(t) = \sum_{j=1}^{N} \mathbf{w}_j \mathbf{c}_j (t - \delta_j), \quad (22)$$

where δ_j is the onset time difference. In our simulation study, particularly the effect of the muscle synergy 2 (δ_2) is evaluated since there was main difference in this synergy.

4.3. Results of Forward Dynamic Simulation

Detailed parameters for our neuromusculoskeletal model can be found in our previous study.[13] Figure 10 shows spatiotemporal patterns of muscle synergies used in our simulation study. They had the same characteristics as the ones from measurement experiment. The first synergy mainly activated RA to bend forward. The second synergy utilized TA, RF, VAS, ES to rise their hip. The third synergy activated most of the muscles to extend the knee and the upper trunk. The fourth synergy activated mostly GAS, SOL, BFS, and GMA to control ankle and hip to stabilize their posture. Similarly, start time and its duration of each synergy is similar to the measurement experiment.

Figure 11 shows the joint kinematics from sitting to standing using different parameters. The vertical direction shows the angles in radian. The horizontal direction shows the motion process (normalized motion time). Figure 11(c) and (d) represent that hip and lumbar joints have larger amplitude when the muscle synergy 2 started 10 or 20% later. The results also indicated that the subjects need to bend their body more to move their CoM forward when using stabilization strategy. These results also showed that the simulation study could generate different strategies using the same spatial patterns.

In our simulation results, the start time of the muscle synergy 2 (δ_2) was changed to 0, 10 and 20%. Figure 12 shows CoM trajectory from sitting to standing using different parameters. The vertical and horizontal displacements were normalized based on the height of the musculoskeletal model. Gray square under the graph shows the feet support area. The results show that the model tends to bend more deeply when the start time of the muscle synergy 2 was delayed. Later the synergy 2 started, the time of upward movement became afterwards. When the muscle synergy 2 started 10 or 20% later, they firstly moved their CoM onto the feet and start moving upward. This corresponds to the characteristics of different strategies reported in the previous study [6] and found in our measurement experiment. The lines with the circle markers indicate CoM trajectories from simulation study. This result also shows that the simulation study could generate different strategies using the same spatial patterns.

5. Discussion

In this study, the muscle synergy model was used to clarify the differences in various strategies in human standing-up motion. The measurement experiment was performed to investigate the muscle synergy structure during standing-up motion. However, analysis of the experiment could only obtained necessary conditions to accomplish the motion. To verify the findings from the measurement experiment, the simulation was employed in this study.

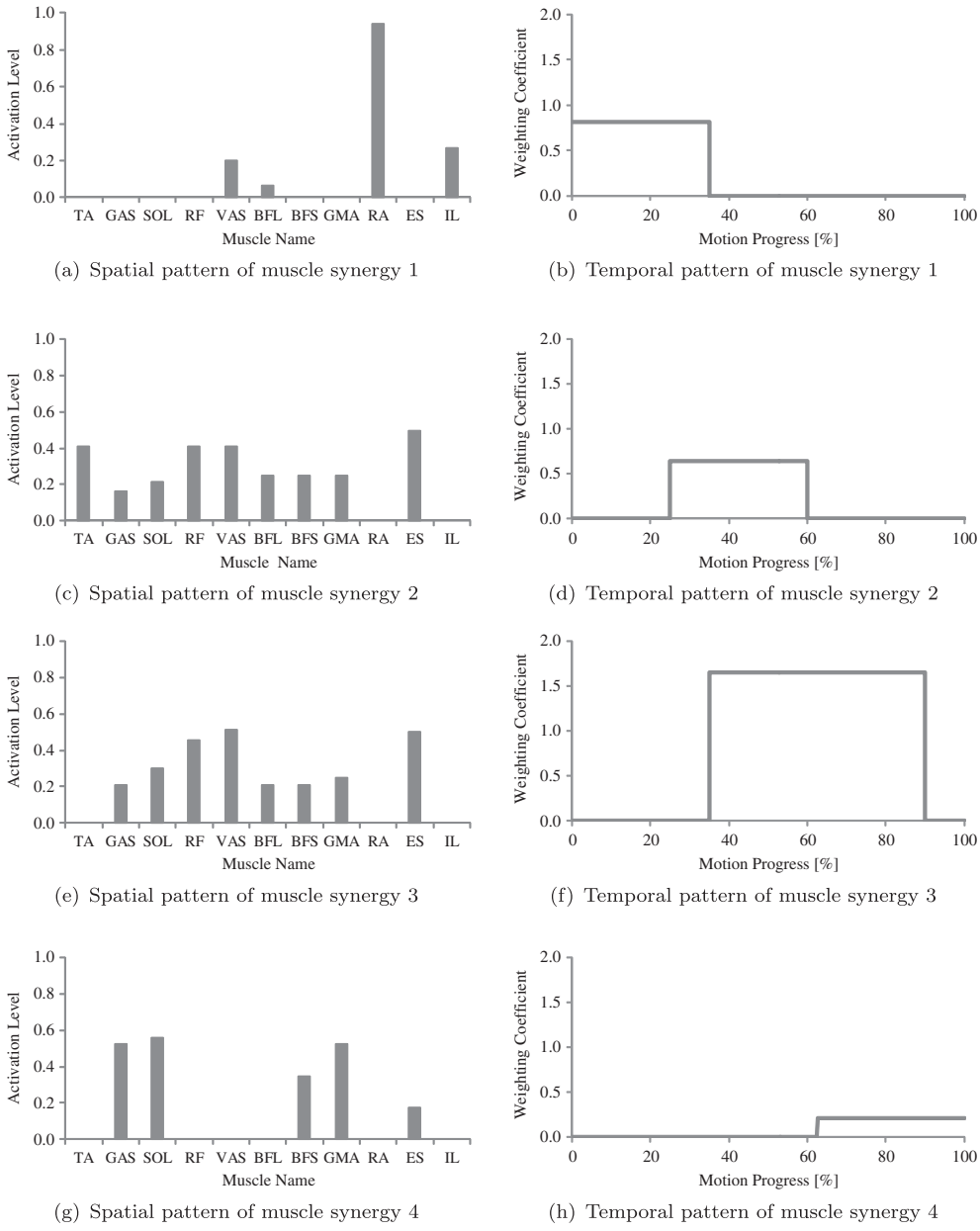

Figure 10. Spatiotemporal patterns of four muscle synergies. Figures (a), (c), (e), and (g) show the spatial patterns of the four muscle synergies. Above bars show the relative activation level of muscles. Figures (b), (d), (f), and (h) show the time-varying weighting coefficient of muscle synergyies 1–4.

Both experimental and simulation results showed that four muscle synergies could successfully represent standing-up motion of the different strategies. For the spatial patterns of measurement experiment shown in Figure 5, both momentum transfer and stabilization strategies have similar spatial patterns of muscle synergies but different temporal patterns. Although the results of the measurement experiment show that the activation levels were different in some muscles among different strategies, two approaches were used to validate that the same spatial patterns could generate the different strategies. The first approach is to calculate the similarity between the each muscle synergies of the two strategies quantified using the cosine principal angles.[18] These results showed that synergies of two strategies were similar each other (more than 0.90). The second method is using the simulation to indicate that only changing the start time can generate different standing-up motion movements. Our simulation results validated that it would be possible to generate different strategies only by changing temporal patterns. Therefore, it can verify that different activation levels in the spatial pattern will not affect the difference of motion strategies. The finding of different temporal patterns implied that all the muscles that are activated during standing-up motion involved dynamic weightings of these basic patterns. The temporal

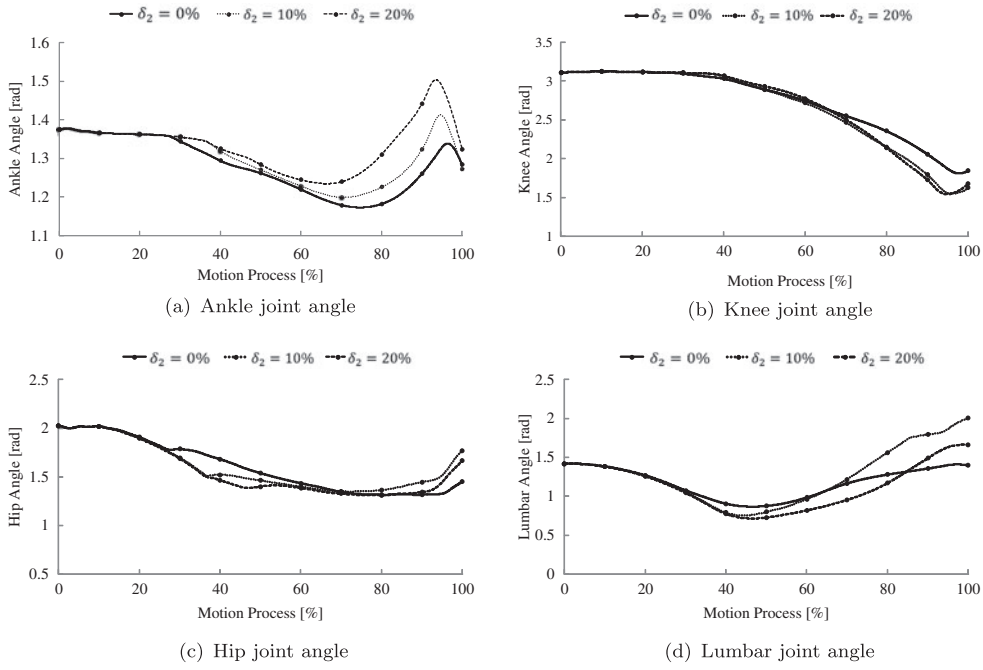

Figure 11. Simulated joint angles. Figures (a)–(d) show ankle, knee, hip, and lumbar joint angles respectively.

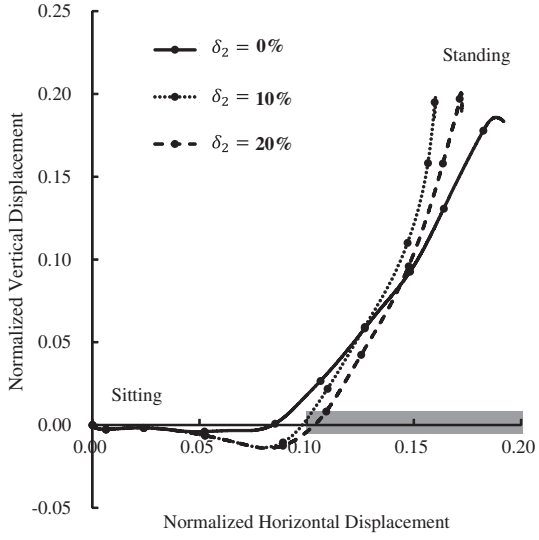

Figure 12. CoM trajectory. Center of mass trajectories at the different start time of muscle synergy 2 (δ_2) are depicted above. These CoM trajectories are generated from our forward dynamic simulation. This shows that humans started upward movement later when the start time of the muscle synergy 2 was delayed. The similar characteristic movement was verified in the simulation study as the measurement experiment.

patterns changed depend on the kinematic and kinetic demands of the movements. In the case of momentum transfer strategy, the start time and peak time are earlier in muscle synergy 2, as shown in Figure 5(d). When the muscle synergy 2 started ealier, the subject began to generate momentum to move upward earlier before the subject moved his/her horizontal CoM onto the feet. On the other hand, when the muscle synergy started later, the subject moved upward after the horizontal CoM moved forward. These characteristics were verified in our simulation study as well. In the simulation, we use the same spatial patterns and the only difference was the start time of the muscle synergy 2. The results of measurement experiment and simulation study showed that there are some difference between the activation levels in spatial patterns, for example, muscle RA in muscle synergy 1 and muscles RA, VAS and ES in muscle synergy 3. One reason for the differences between simulation and measure experiment results in spatial patterns such as muscle RA was that inner muscles contributed more than RA, and therefore only low activation was found in measured data. However, it was ensured that muscle synergy could generate enough muscle activation to flex their HAT. For muscle synergy 3, muscles BFL, BFS, and ES are mainly activated for extending the body. But inner muscles which are not measured in this study may also contribute more than these muscles. Therefore the activation level of these muscles in simulation results is higher than that of the measurement experiment results. This results generated by changing the temporal patterns also supports the finding from the measurement experiment. By combining the two methodologies, this study clarified how humans coordinate their muscles to generate standing-up motion using different strategies. It could be implied that this different start times caused different strategies.

In our previous study,[13] we firstly hypothesized that by changing the start time of muscle synergy 3, the simulation model could generate different standing-up movements. The simulation model only employed the reaction force, body kinetic data, and muscle activation data from one subject. Therefore, it could only analyze the necessary condition (the start time of muscle synergy 3) for standing-up motion. However in this study, we conducted the measurement experiment to elucidate the essential condition for standing-up motion using different strategies. The results showed that by changing the start time of muscle synergy 2, different standing-up strategies could be generated.

Similar characteristics of standing-up movements were also reported in previous study.[6] This literature found three strategies (momentum transfer, stabilization, and hybrid) used in humans standing-up motion which generate different movements.[6] When using the stabilization strategy, the moment arm of the body CoM is shorter than that of the momentum transfer strategy. Therefore, the required joint torque is lower in stabilization than momentum transfer strategy. The main function of muscle synergy 2 is to rise the hip by activating muscle TA, RF, and VAS. Therefore, stabilization strategy is achieved when the muscle synergy 2 started later to have longer period of moving forward. Although the CoM results in both simulation and measurement were not similar, they had the same characteristics. When the subjects employed momentum transfer strategy, the subjects started to move the CoM upward before it reached the feet position in the measurement, as in Figure 3. The simulation result had similar characteristics. When $\delta_2 = 0\%$, the CoM also moved upward before moved forward to reach the feet position, as in Figure 12. When the subjects employed stabilization strategy, the subject moved CoM to reach the feet position firstly, then started to move it upward, as shown in Figure 3. The simulation results in Figure 12 also have similar characteristics. When $\delta_2 = 10\%$ and $\delta_2 = 20\%$, the subjects firstly moved the CoM on their feet, then started to move upward. Therefore, these results indicated that both measurement experiment and simulation study generated the similar CoM trajectories when the same standing-up motion strategy was employed.

The joint kinematics also represented the similar characteristics in the CoM trajectories between the measurement experiment and simulation study. In the joint kinematics results of both experiment and simulation, the amplitudes of hip and lumbar joints were larger when the subjects employed the stabilization strategies than that of momentum transfer strategies. The larger amplitudes of the hip and lumbar joints indicated that the subjects need to bend their body more to move their CoM on their feet when they used the stabilization strategy. However, the joint kinematics still had some differences in the ankle joint. The ankle joint angles are different between experiment and simulation results. One reason for this is because of postural control in our simulation model. In the simulation, a simple proportional controller was used to follow the target trajectory, and the same kinematics was used as a reference movement. However, they might require additional postural controller to stabilize and keep their CoM on the feet for the ankle joint especially in the stabilization strategy. Further postural controller will be considered and investigated between two strategies.

The obtained results contribute to evaluate the effectiveness of the rehabilitation and assistive robots. Extracted muscle synergy structure and their difference among strategies can be used as target state of the devices. To evaluate the effectiveness of the rehabilitation or assistive robots, the muscle synergy structure could provide useful information. In the rehabilitation of the patients and training of the older adults, they should not rely too much on the assistive robots, but they should enhance their physical ability. It would be possible to evaluate if the users of the assistive robots can appropriately utilize muscle synergy without relying too much on the device.

6. Conclusions

In this study, muscle synergy model was used to analyze how humans control their muscles to generate standing-up motion using different strategies. The measurement experiment was performed to analyze observed phenomena and necessary conditions to generate standing-up motion. In addition, the simulation study was conducted to verify the outcome of the experiment. Both simulation and experiments verified that four muscle synergies could successfully represent human standing-up motion. From their results, it was found that the spatial pattern of the muscle synergies changed little even when the strategies changed. However, humans adaptively control the parameter (start time) of the synergy to achieve different strategies of the standing-up motion.

Disclosure statement

No potential conflict of interest was reported by the authors.

Funding

This work was supported by JSPS KAKENHI [grant number 15K20956], [grant number 26120005], [grant number 16H04293]; CASIO Science Promotion Foundation and JST RISTEX Service Science, Solutions and Foundation Integrated Research Program.

Notes on contributors

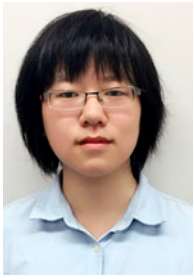

Ningjia Yang received the bachelor degree from Nankai University, China in 2014. She is currently a master student in the Department of Precision Engineering at the University of Tokyo. Her research interests are rehabilitation robotics and human biomechanics.

Qi An received his BE, ME and PhD in Engineering from the University of Tokyo in 2009, 2011 and 2014 respectively. From 2012, he is a JSPS Research Fellowship for Young Scientists (DC1). He is currently an assistant professor in the Department of Precision Engineering at the University of Tokyo and a visiting researcher in RIKEN from 2015. His research interests are rehabilitation robotics and human biomechanics. He is a member of RSJ, SICE, and IEEE.

Hiroshi Yamakawa received BE, ME from the Department of Electrical and Information Engineering, University of the Ryukyus, in 1985, 1987, respectively. He has been working as a technical staff at the Faculty of Engineering, University of Tokyo since 1992. He received PH.D at the University of Tokyo in 2006. His research interests are mechatronics, robotics, microdynamics and biosensing. He is a member of RSJ, SICE, JSPE and IEICE.

Yusuke Tamura received his BE, ME, and PhD degrees in Engineering in 2003, 2005, and 2008 respectively from the University of Tokyo. From 2006 to 2008, he was a Research Fellow of the Japan Society for the Promotion of Science. He worked as a Project Researcher of the University of Tokyo from 2008 to 2012 and an Assistant Professor of Chuo University, Japan from 2012 to 2015. He is currently a Project Associate Professor in the Department of Precision Engineering, the University of Tokyo. His research interests include human-robot interaction, remote control technology, and sports engineering. He is a member of IEEE, JSME, and RSJ.

Atsushi Yamashita is an associate professor in Department of Precision Engineering, the University of Tokyo, Japan. He received BE, ME and PhD from Department of Precision Engineering, the University of Tokyo, in 1996, 1998, and 2001, respectively. From 1998 to 2001, he was a junior research associate in RIKEN (Institute of Physical and Chemical Research). From 2001 to 2008, he was an assistant professor of Shizuoka University. From 2006 to 2007, he was a visiting associate of California Institute of Technology. From 2008 to 2011, he was an associate professor of Shizuoka University. From 2011, he is an associate professor in Department of Precision Engineering, the University of Tokyo. His research interests are robot vision, image processing, and intelligent sensing for robots. He is a member of ACM, IEEE, JSPE, RSJ, IEICE, JSME, IEEJ, IPSJ, ITE and SICE.

Hajime Asama received his MS and Dr Eng. in Engineering from the University of Tokyo, in 1984 and 1989, respectively. He was a Research Scientist, etc. in RIKEN Japan from 1986 to 2002. He became a professor of RACE, the University of Tokyo in 2002, and a professor of School of Engineering, the University of Tokyo since 2009. He received RSJ Distinguished Service Award in 2013, etc. He was the vice-president of Robotics Society of Japan in 2011–2012. an AdCom member of IEEE Robotics and Automation Society in 2007–2009, the president of International Society for Intelligent Autonomous Systems from 2014, an associate editor of Journal of Robotics and Autonomous Systems, etc. He is a Fellow of JSME and RSJ. His main research interests are distributed autonomous robotic systems, smart spaces, service engineering, embodied brain systems, service robotics, and disaster response robots.

References

[1] United Nations, Department of Economic and Social Affairs, Population Division. World population ageing 2013. ST/ESA/SER.A/348; 2013.

[2] Chugo D, Okada E, Kawabata K, et al. Force assistance system for standing-up motion. Ind. Robot: Int. J. 2007;34:128–134.

[3] Agrawal SK, Caltim G, Fattah A, et al. Design of a passive gravity-balanced assistive device for sit-to-stand tasks. J. Mech. Des. Trans. ASME. 2006;128:1122–1129.

[4] Kawanishi R, Hasegawa Y, Tsukahara A, et al. Sit-to-stand and stand-to-sit transfer support for complete paraplegic patients with robot suit HAL. Adv. Rob. 2010;24:1615–1638.

[5] Matjacic Z, Zadravec M, Oblak J. Sit-to-stand trainer: an apparatus for training 'normal-like' sit to stand movement. IEEE Trans. Neural Syst. Rehabil. Eng. 2015;99:1–10.

[6] Hughes MA, Weiner DK, Schenkman ML, et al. Chair rise strategies in the elderly. Clin. Biomech. 1994;9:187–192.

[7] Wheeler J, Woodward C, Ucovich RL, et al. Rising from a chair influence of age and chair design. Phys. Ther. 1985;65:22–26.

[8] Bernstein N. The coordination and regulation of movement. Oxford: Pergamon; 1967.

[9] Ivanenko YP, Poppele RE, Lacquaniti F. Five basic muscle activation patterns account for muscle activity during human locomotion. J. Physiol. 2004;556:267–282.

[10] Torres-Oviedo G, Ting LH. Muscle synergies characterizing human postural responses. J. Neurophysiology. 2007;2007:2144–2156.

[11] Weiss EJ, Flanders M. Muscular and postural synergies of the human hand. J. Neurophysiology. 2004;92:523–535.
[12] Carson RG. Changes in muscle coordination with training. J. Appl. Physiol. 2006;101:1506–1513.
[13] An Q, Ishikawa Y, Aoi S, et al. Analysis of muscle synergy contribution on human standing-up motion using human neuro-musculoskeletal model. Proceedings of the 2015 IEEE International Conference on Robotics and Automation (ICRA2015); Seattle; 2015; p. 5885–5890.
[14] Aoi S, Ogihara N, Funato T, et al. Evaluating functional roles of phase resetting in generation of adaptive human bipedal walking with a physiologically based model of the spinal pattern generator. Biol. Cybern. 2010;102:373–387.
[15] Jo S, Massaquoi SG. A model of cerebrocerebello-spinomuscular interaction in the sagittal control of human walking. Biol. Cybern. 2007;96:279–307.
[16] Berry MW, Browne M, Lagnville AN, et al. Algorithms and applications for approximate nonnegative matrix factorization. Comput. Stat. Data Anal. 2006;52:155–173.
[17] Schenkman M, Berger RA, Riley PO, et al. Whole-body movements during rising to standing from sitting. Phys. Ther. 1990;70:638–648.
[18] Cheung VCK, Piron L, Agostini M, et al. Stability of muscle synergies for voluntary actions after cortical stroke in humans. Proc. Nat. Acad. Sci. 2009;106:19563–19568.
[19] Ogihara N, Yamazaki N. Generation of human bipedal locomotion by a bio-mimetic neuro-musculo-skeletal model. Biol. Cybern. 2001;84:1–11.
[20] Christophy M, Senan NAF, Lotz JC, et al. A musculoskeletal model for the lumbar spine. Biomech. Model. Mechanobiol. 2012;11:19–34.
[21] Zajac FE. Muscle and tendon: properties, models, scaling, and application to biomechanics and motor control. Crit. Rev. Biomed. Eng. 1989;17:359–411.
[22] Hatze H. Myocybernetic control models of kkeletal muscles. Biol. Cybern. 1977;25:103–119.
[23] Pandy MG, Zajac FE, Sim E, et al. An optimal control model for maximum-height human jumping. J. Biomech. 1990;30:1185–1198.
[24] Thelen DG. Adjustment of muscle mechanics model parameters to simulate dynamic contractions in older adults. ASME J. Biomech. Eng. 2003;125:70–77.
[25] Winters JM. An improved muscle-reflex actuator for use in large-scale neuromusculoskeletal models. Ann. Biomed. Eng. 1995;23:359–374.
[26] Neptune RR, Kautz SA. Muscle activation and deactivation dynamics: the governing properties in fast cyclical human movement performance? Exercise Sport Sci. Rev. 2001;29:76–81.
[27] Kuo P, Deshpahde AD. Contribution of passive properties of muscle-tendon units to the metacarpophalangeal joint torque of the index finger. Proceedings of the 2010 IEEE RAS&EMBS International Conference on Biomedical Robotics and Biomechatronics (BioRob2010); 2010; Tokyo; p. 288–294.